



## Short communication

## Development of lithium-ion battery for fuel cell hybrid electric vehicle application

T. Kojima<sup>a</sup>, T. Ishizu<sup>a</sup>, T. Horiba<sup>a,\*</sup>, M. Yoshikawa<sup>b</sup><sup>a</sup> Hitachi Vehicle Energy, Ltd., 2200 Oka, Fukaya, Saitama 369-0297, Japan<sup>b</sup> Hitachi Research Laboratory, Hitachi, Ltd., 7-1-1 Ohmikacho, Hitachi, Ibaraki 319-1292, Japan

## ARTICLE INFO

## Article history:

Received 31 July 2008

Received in revised form 2 October 2008

Accepted 15 October 2008

Available online 5 November 2008

## Keywords:

Lithium-ion battery

Fuel cell vehicle

Specific energy

Specific power

10–15 mode

## ABSTRACT

We participated in a national project, to develop lithium batteries for use in fuel cell hybrid electric vehicles (FCHEVs), etc., in Japan as a battery developer. The lithium battery in an FCHEV system has to supply the system with not only power but also energy.

We have developed an elliptic single cell, a 4-cell module, and an application-specific integrated circuit to monitor and control the cells. Our developed single cell has achieved a specific energy of  $83 \text{ Wh kg}^{-1}$ , a specific power output of  $3380 \text{ W kg}^{-1}$  at 50% state of charge (SOC) for 10 s. The performance of the 3 kWh pack was evaluated using the 4-cell module data: the specific energy was  $75 \text{ Wh kg}^{-1}$  and specific power output was  $2250 \text{ W kg}^{-1}$ . Introduction of a lithium-ion battery into the FCHEV definitely suggested a reduced fuel consumption to 2/3 of that without the lithium-ion battery based on our measurements and calculations for the 10–15 driving mode.

© 2008 Elsevier B.V. All rights reserved.

## 1. Introduction

One of the most serious issues in the 21st century is how to compromise the increasing demand for energy and the environment. As for the carbon dioxide emission, for example, it has increased up to five times that of 100 years ago, and its concentration is also increasing. For oil consumption by sectors, the transportation sector consumes more than half of the total, therefore, an improved fuel economy of vehicles is inevitable in order to reduce carbon dioxide emissions for coping with this global environmental issue. Consequently, electrified vehicles such as electric vehicles (EVs), hybrid electric vehicles (HEVs), and fuel cell hybrid electric vehicles (FCHEVs) are expected to be key technologies to fight this issue.

A 5-year national project, from FY 2002 to 2006, in Japan, the “Development of Lithium Battery Technology for Use by Fuel Cell Vehicles,” was completed in March 2007 [1]. The purpose of the project was to develop lithium batteries for use in fuel cell vehicles, etc. Project members were classified into three groups: battery developers, fundamental technology, and new material developers. We, Hitachi and Hitachi Vehicle Energy, participated in the project as a battery developer.

The lithium battery in an FCHEV system has to undertake three functions: first, the energy source for EV driving during fuel cell pre-heating, second, power assist in acceleration, and third, regeneration during deceleration. The fuel cell system demands not only power but also energy to meet these functions and to complement the low flexibility of the fuel cell stack power capability.

The target for the project is shown in Table 1. [2] These target values are those for a 3 kWh battery pack: a  $1800 \text{ Wh kg}^{-1}$  specific power,  $70 \text{ Wh kg}^{-1}$  specific energy, 15-year life, etc. Therefore, the cells to form the module or the pack should have much higher values of specific power and specific energy than those for the 3 kWh battery pack listed in this table.

We have developed an elliptic single cell, a 4-cell module, and an application-specific integrated circuit to monitor and control the cells. The detailed results are described as follows.

## 2. Experimental

The cell chemistry of the lithium-ion battery consists of a positive electrode of a manganese-based material and a negative electrode of a hard carbon–graphite composite. Both electrodes were formed by coating slurry containing the active material with some conductive materials and a binder on a metal foil substrate, i.e., aluminum for the positive electrode and copper for the negative electrode. The electrolytic solution consisted of a 1 molar solution of lithium hexafluorophosphate dissolved in a mixture of

\* Corresponding author. Tel.: +81 48 546 1107; fax: +81 48 546 1138.  
E-mail address: [t.horiba@shinkobe-denki.co.jp](mailto:t.horiba@shinkobe-denki.co.jp) (T. Horiba).

**Table 1**  
Target for the national project.

Capacity	3 kWh
Power density	1800 W kg <sup>-1</sup>
Energy density	70 Wh kg <sup>-1</sup>
Life	15 years
Battery cost	50,000 ¥ kWh <sup>-1</sup>
Safety	Durable under abuse conditions and vehicle use environment

organic carbonate solvents. The separator was an ordinary polyolefin microporous sheet.

The positive electrode, the separators and the negative electrode were wound into a flat electrode assembly to form an elliptic cell. This assembly was put into a nickel-plated steel can, and crimped with a gasket and a top cap after injection of the electrolytic solution. We introduced a unique crimp seal technique specific for this elliptic structure. The cell is 108 mm wide, 34 mm deep, and 117 mm high, and the designed capacity was 18.4 Ah.

The rated capacity for the cell was measured at 25 °C at a discharge current of 1/3 CA down to 2.7 V after CC–CV(constant current–constant voltage) charging at a 1/2 CA constant current up to 4.25 V of constant voltage for a total of 2.5 h. We determined the state of charge (SOC)-input/output power diagram, to evaluate the power capability of the high power density cell and a 4-cell module. This method is a kind of extrapolation of the *I*–*V* curves as described in our previous paper in detail [3,4].

### 3. Results and discussion

#### 3.1. Development of single cell

Since we had to develop a lithium-ion battery with both a high specific energy and high specific power for the FCHEV application, we developed a composite anode consisting of a hard carbon and a graphite. The packing density and discharge voltage were enhanced and the charge retention for the first cycle was improved by the addition of graphite, while this addition reduced the specific power. Based on some preliminary test results, we selected the composition of 65% hard carbon and 35% graphite to improve the performance.

Table 2 shows the specifications for the developed single cell. The positive electrode consists of a manganese-based active material, and the negative electrode consists of a mixture of hard carbon and graphite. The rated capacity is 18.4 Ah, the nominal voltage is 3.6 V, the specific energy is 83 Wh kg<sup>-1</sup>, the specific power input at 50% SOC for 10 s is 3010 W kg<sup>-1</sup>, and the specific power output at 50% SOC for 10 s is 3380 W kg<sup>-1</sup>. Fig. 1 is a photo of the single cell, which has a top cap with a positive terminal and a gas release vent on it. The cap is insulated and sealed by a rubber gasket. Therefore, the polarity of the cell casing is negative.

Fig. 2 shows the charge–discharge characteristic of the developed cell. The operating voltage of the medium SOC is raised by the addition of graphite to the negative electrode, which results in the increased specific energy. We also measured the discharge

**Table 2**  
Specifications of the developed single cell.

Positive electrode	Mn-based
Negative electrode	Amorphous/graphite
Rated capacity	18.4 Ah
Nominal voltage	3.6 V
Specific energy	83 Wh kg <sup>-1</sup>
Specific power input @ 50% SOC	3010 W kg <sup>-1</sup>
Specific power output @ 50% SOC	3380 W kg <sup>-1</sup>



Fig. 1. Photo of developed cell.

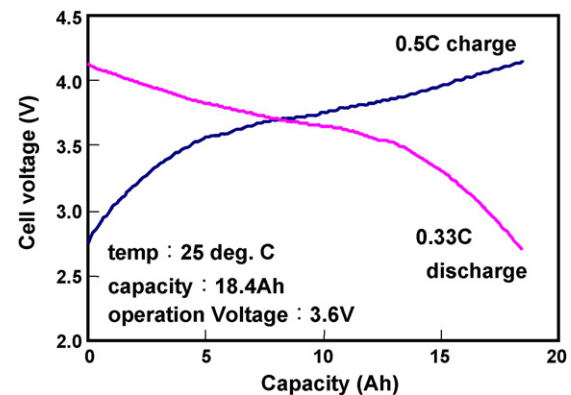


Fig. 2. Charge–discharge characteristics of the developed cell.

rate and low temperature characteristics of the cell. It showed a good high rate discharge capability, namely, the discharge capacity at 10C maintained 93% of that at 0.33C. Reducing the temperature to 0 °C did not show any significant discharge capacity loss, while the discharge capacity at –20 °C showed around a 16% loss. This change was probably caused by the increased internal resistance.

We evaluated the specific power by extrapolating the 10 s current to 4.25 V for charging and 2.5 V for discharging. This result is shown in Fig. 3. The enhanced operating voltages by graphite also raised the power capability, and these results showed a well-balanced power capability in a symmetrical form between the input and output.

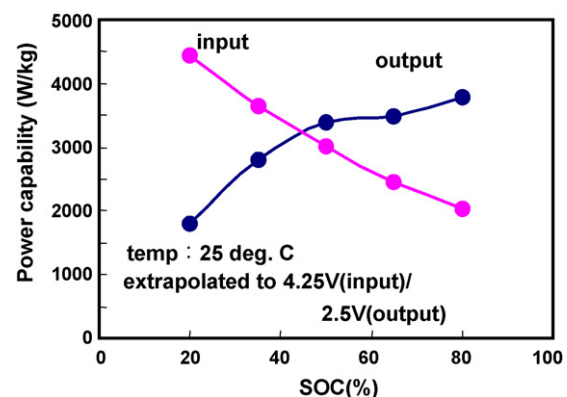


Fig. 3. 10-s power capability of the developed cell.

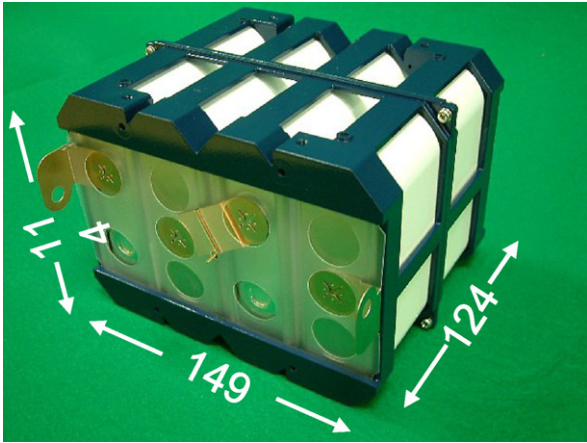


Fig. 4. Photo of the developed 4-cell module.

**Table 3**  
Specifications of the 4-cell module.

Capacity	18.4 Ah
Operating voltage	14.4 V
Specific energy	80 Wh kg <sup>-1</sup>
Volumetric energy density	126 Wh L <sup>-1</sup>
Specific power output @ 50% SOC	2400 W kg <sup>-1</sup>
Specific power input @ 50% SOC	2120 W kg <sup>-1</sup>

### 3.2. 4-Cell module

Our 4-cell module is shown in Fig. 4. Four single cells, alternatively turned by 90° in opposite directions, are connected in series with copper-clad nickel bus bars and installed in a framework made of a polymer material. The cooling gap between the two cells was optimized for air-cooling by using thermal simulation. The strength of the module framework was also validated through simulation for mechanical stress and vibration, other than the vibration and shock test.

Table 3 shows the specifications for the 4-cell module, which was designed and developed as a component unit of a 3 kWh battery pack. Its capacity is 18.4 Ah, which is the same as that for the single cells, because of the serial connection. The operating voltage is 14.4 V, which is four times that of the single cell. The specific energy and specific power capabilities are also shown. These specific energy and powers are lower than those for the single cell due to the weight of the bus bars and the framework, and the electric resistance of the bus bar connection.

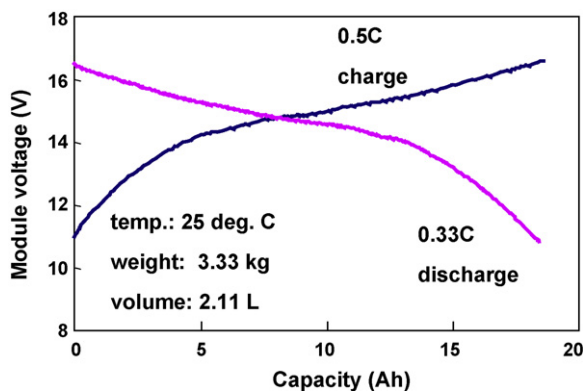


Fig. 5. Charge–discharge characteristics of the 4-cell module.

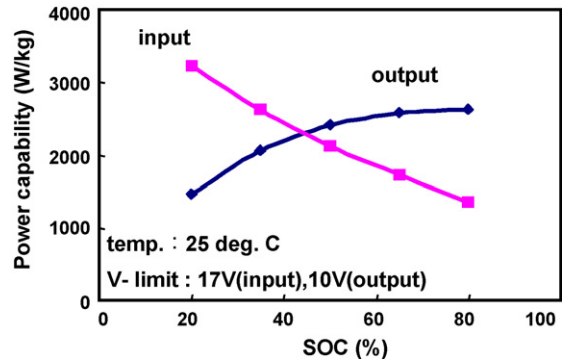


Fig. 6. 10-s power capability for the 4-cell module.

Fig. 5 shows the charge/discharge characteristic of the 4-cell module, which has almost the same shape as that for the single cell, but the voltage is multiplied by 4. The discharge capacity was 18.4 Ah and the average discharge voltage was 14.4 V, the mass was 3.33 kg and the volume was 2.11 L, which figured out to be 80 Wh kg<sup>-1</sup> and 126 Wh L<sup>-1</sup>. We accomplished a specific energy of 80 Wh kg<sup>-1</sup> with a minimum loss in forming a module from four single cells.

Fig. 6 shows the 10-s power capabilities of the 4-cell module: 2400 W kg<sup>-1</sup> for output at 50% SOC and 2120 W kg<sup>-1</sup> for input at 50% SOC, which also shows a profile similar to that for the single cell, though the specific values are slightly lower due to the additional weight and the resistance mentioned above.

### 3.3. Abuse and durability tests

We conducted an abuse test and durability test. The abuse test involved overcharge, overdischarge, short circuit, nail penetration, and crushing. Table 4 summarizes the test conditions and the results. Although the emissions of smoke and solvent vapor were observed during the nail penetration and crush test, no fire or rupture was observed during the all abuse testing, which proved good safety record.

The vibration test as a durability test was conducted using the 4-cell module. No loss of capacity was observed after the vibration

**Table 4**  
Abuse and durability tests.

Items	Condition	Smoke	Fire	Rupture
Abuse (cell)				
Over-charge	Charge up to 200% SOC at 2 C	No	No	No
Over-discharge	Discharge down to 0 V at 2 C	No	No	No
Short circuit	Short with a circuit less than 5 mΩ at 100% SOC	No	No	No
Penetration	Penetrate with a Ø5 mm steel nail at 100% SOC	Yes	No	No
Crush	Crush with a Ø20 mm cylinder to 50% thickness at 100% SOC	Yes	No	No
Durability (4-cell MD)				
Vibration	7–200 Hz continuous, along X, Y, and Z-axis for 3 h, in 8 G; measure capacity before and after the vibration		Before/after = 18.45 Ah/18.44 Ah	

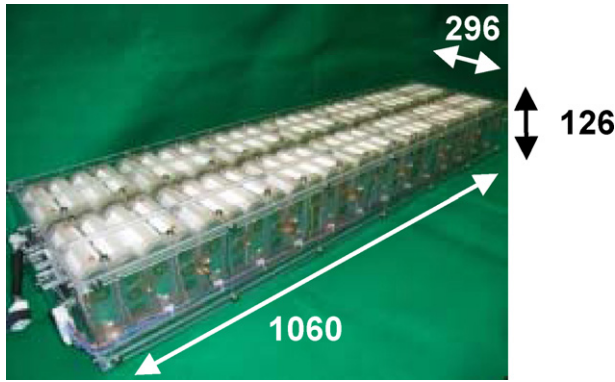


Fig. 7. Mock-up of 3 kWh battery pack.

based on the conditions shown in Table 4. Good durability was also confirmed.

### 3.4. Control system

A battery control system is very important for the lithium-ion battery system not only for safety, but also for long life and energy efficiency. Moreover, a compact and high reliability control system is essential for optimization of the battery pack. We have been developing a cell control system with ASIC, an application-specific integrated circuit, based on this concept [5–7].

We modified the control algorithm for vehicle application to make it fit the FCHEV system and our lithium-ion batteries. The result showed that the SOC estimation accuracy of the control algorithm was improved. We also developed new ASIC specifications to improve its performance, and experimentally manufactured the new ASIC version. The ASIC showed a sufficient performance to meet the specifications we had designed. These results definitely contributed to reducing the mass and volume during the design of the 3 kWh battery pack.

### 3.5. Pack design

Our 3 kWh pack design consists of fourteen 4-cell modules, that is, 56 cells in total. Simulations for structure strength and thermal management were conducted to optimize the pack design. Fig. 7 shows a mock-up of the 3 kWh battery pack containing 56 empty cells. The framework is made of polymer materials. The cooling air duct is formed in the bottom plate. The ASIC cell controller is attached to the left end face of the pack case in Fig. 7.

In the NEDO project, the 3 kWh pack performance was to be evaluated on the basis of the module performance. Therefore, we utilized the weight and volume data measured using the 3 kWh pack mock-up along with the performance data for the 4-cell module shown in Table 3, Fig. 5 and Fig. 6. The result is summarized in Table 5. We achieved a  $75 \text{ Wh kg}^{-1}$  specific energy and  $2250 \text{ W kg}^{-1}$

Table 5  
Calculation for 3 kWh pack.

Items	Meas.	Target
Mock-up		
Frame weight (kg)	2.9	–
Total weight (kg)	47.7	–
Total volume (L)	39.5	–
Calc. value		
Specific energy ( $\text{Wh kg}^{-1}$ )	75	70
Specific power output @ 50% SOC ( $\text{W kg}^{-1}$ )	2250	1800

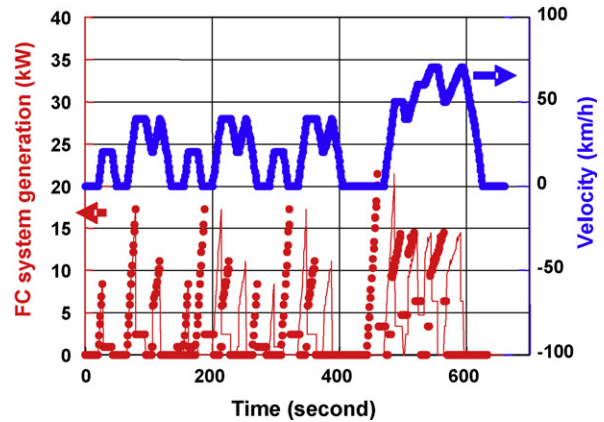


Fig. 8. Energy requirement by FC system during 10–15 mode operation.

specific power output at 50% SOC, which are sufficiently higher than the target values for the project shown in Table 1.

### 3.6. Simulation on onboard conditions

We evaluated the merits of equipping an FCHEV with a lithium battery. The 10–15 mode, which is a Japanese standard driving cycle, was adopted as the car driving cycle on the FCHEV system. Fig. 8 shows the mode in velocity in the upper half of the figure, and the velocity of the car is transformed into a power requirement for the FCHEV system as shown in the lower half [8]. The prerequisites to share the power requirement with the FC stack and lithium battery are as follows:

- (i) Capacity of the battery is reduced to 1 kWh for normalization.
- (ii) Velocity of not less than  $10 \text{ km h}^{-1}$  is regenerated during braking.
- (iii) The FC load is kept around the middle range.

We divided the load of the FCHEV for the 10–15 mode into the fuel cells, and lithium-ion batteries, according to this prerequisite. We then applied the divided load for a lithium-ion battery to it and measured the electric power balance, and estimated the improvement of fuel economy between the system with and without the

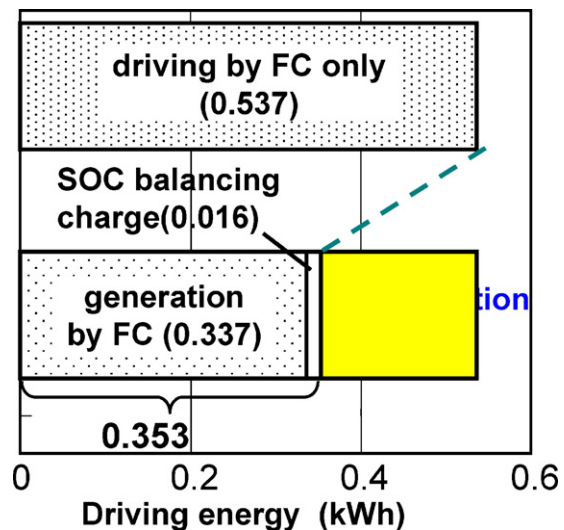


Fig. 9. Merits of developed battery for FC system.

lithium-ion battery. Fig. 9 shows this result and explicitly indicates the advantage of the FC system with the developed lithium-ion battery. If driving by FC only, 0.537 kWh is consumed in one cycle, while the introduction of our lithium-ion battery reduces the energy consumption to 0.353 kWh because of the regeneration energy during braking. This equals to 2/3 of that for the FC system without the lithium-ion battery, which is a significant fuel economy improvement.

#### 4. Conclusion

We have achieved a specific energy of  $83 \text{ Wh kg}^{-1}$ , a specific power output of  $3380 \text{ W kg}^{-1}$  at 50% SOC for 10 s with our developed single cell. The performance of the 3 kWh pack was evaluated using the 4-cell module data: the specific energy was  $75 \text{ Wh kg}^{-1}$  and specific power output was  $2250 \text{ W kg}^{-1}$ . Both of them surpassed the target of the NEDO project. Introduction of a lithium-ion battery into the FCHEV definitely suggested a reduced fuel consumption to 2/3 of that without the lithium-ion battery based on our measurements and calculations for the 10–15 driving mode. Namely, it was quantitatively proved that our lithium-ion battery is an excellent technology to support FCHEV systems.

A further reduction in weight and volume is necessary in order to apply lithium-ion batteries to various uses other than the FCHEV.

Moreover, an improved reliability is essential for the extensive application in the market: accumulation of more performance data of a lithium-ion battery under various conditions, enhancement of life prediction by storing much more life test data.

#### Acknowledgements

This work was sponsored by NEDO (New Energy & Industrial Technology Development Organization) as a part of a national project in Japan. We heartily acknowledge all the people who participated in the project.

#### References

- [1] M. Daito, *Electrochemistry* 71 (2003) 135–137.
- [2] T. Ikeya, H. Miyazaki, H. Kuriyama, T. Sato, *Proceedings of the 21st International Electric Vehicle Symposium, Monaco, April 2–6, 2005*.
- [3] T. Horiba, T. Maeshima, T. Matsumura, M. Koseki, J. Arai, Y. Muranaka, *J. Power Sources* 146 (2005) 107–110.
- [4] *FreedonCAR Battery Test Manual for Power Assist Hybrid Electric Vehicles, DOE/ID-11069, October 2003*.
- [5] A. Emori, A. Kudou, *Proceedings of 5th International Automotive Battery & Ultracapacitor Conference, Honolulu Hawaii, June, 15–17, 2005, Abstract*.
- [6] A. Emori, A. Kudou, T. Horiba, *Tanso* 229 (2007) 261–266.
- [7] T. Horiba, *J. Power Sources* 174 (2007) 981–984.
- [8] K. Otsuka, E. Kuroda, S. Watanabe, *JARI Res. J.* 26 (6) (2004) 23–26.